Journal of Natural Gas Science and Engineering 20 (2014) 328–336

Contents lists available at ScienceDirect

Journal of Natural Gas Science and Engineering

journal homepage: www.elsevier.com/locate/jngse

CMM capture engineering challenges and characteristics of in-situ stress distribution in deep level of Huainan coalfield

Qingquan Liu [a], Yuanping Cheng [a, *], Liang Yuan [a, b], Bi Tong [b], Shengli Kong [a], Rong Zhang [a]

[a] National Engineering Research Center for Coal Gas Control, China University of Mining & Technology, Xuzhou 221116, China
[b] Huainan Mining Group Co., Ltd., Huainan 232001, China

ARTICLE INFO

Article history:
Received 18 May 2014
Received in revised form
25 June 2014
Accepted 26 June 2014
Available online 5 August 2014

Keywords:
Huainan coalfield
Coal mine methane
Underground opening instability
In-situ stress distribution

ABSTRACT

CMM (coal mine methane) capture engineering faces many challenges in the deep levels of Huainan coalfield. The instabilities of roadways and drainage boreholes induced a very low CMM capture efficiency. In-situ stress distribution is one of the most important and fundamental factors affecting the stability of underground openings. Knowledge of the characteristics of in-situ stress distribution in Huainan coalfield is very important when dealing with the design and construction of drainage boreholes. The in-situ stress measurement results of 74 test sites in 13 coal mines of Huainan coalfield have been evaluated and analyzed to further our understanding of these issues. Generally, the in-situ stress field of Huainan coalfield at a depth range of 350–1100 m belongs to the tectonic stress field; the maximum and minimum principal stresses are mainly horizontal stresses, and the intermediate principal stress is mainly a vertical stress; the orientation of the horizontal principal stress is mainly along the NEE–EW direction. Coefficients of lateral stress range between 0.51 and 1.82, this range decreases gradually with depth and approaches 1.0, implying that hydrostatic pressure may occur at deep levels of Huainan coalfield. Coefficients of average lateral stress are from 0.48 to 1.44; their regression curve falls between the Hoek–Brown outer envelope and the Hoek–Brown median envelope.

1. Introduction

With expanding economic development and the growing demand for energy, coal will remain the main energy source in China well into the future (Yuan, 2008). Annual coal production in China in 2013 was approximately 3.7 billion tons, which is approximately 70% of the primary energy in China and approximately 40% of the world's coal consumption. After ten years of rapid development, the mining depths of some coal mines in central and east China now reach between 800 m and 1200 m; the vertical stress of the coal seams is in the range of 22–33 MPa (Kang et al., 2010); the gas pressure and gas content can reach 6 MPa and 22 m^3/t, respectively (Wang et al., 2012a). Moreover, the coal seams in the deep levels are quite soft and are characterized by low strength and low permeability. Coal mine methane (CMM) capture engineering faces many opportunities and challenges arising from these characteristics (Li and Fu, 2006; Yao et al., 2009).

Coal mine methane is a general term for all methane released mainly during and after mining operations (Karacan et al., 2011). There are three primary reasons for recovering CMM, including increasing mine safety, improving mine economics and benefiting the global and local environment (Bibler et al., 1998, 2014; Wan, 2013). In most Chinese coal mines, capturing CMM by various types of boreholes, which can be drilled in roadways, is the principal recovery method. According to an incomplete statistical record, more than 10,000 km of roadways are excavated annually in China, with 80% of these in coal seams (Kang et al., 2010).

CMM capture efficiency is determined by the stabilities of the roadways and drainage boreholes. The relationship between the stability of underground openings and in-situ stress distribution has been widely studied in recent years (Martin et al., 2003; Bell, 2003; Moos et al., 1998; Peška and Zoback, 1995; Luo et al., 2010, 2011; Zhang et al., 2008). In general, stability problems generated by in-situ stress in various underground openings become more prevalent with depth. Knowledge of the state of in-situ stress in the Earth's crust is very important when dealing with rocks in civil, mining, and energy engineering, as well as in geology and geophysics (Zang et al., 2010). Various methods, which can be

* Corresponding author. Tel.: +86 516 83885948; fax: +86 516 83995097.
E-mail address: cumtcyp@gmail.com (Y. Cheng).

http://dx.doi.org/10.1016/j.jngse.2014.06.025
1875-5100/

classified into two categories, exist for the determination of in-situ stress; the first consists of methods that disturb the in-situ rock conditions, i.e., by inducing strains, deformations or crack openings; the second consists of methods based on the observation of rock behavior without any major influence from the measuring method (Ljunggren et al., 2003). In this study, the stress data of Huainan coalfield was obtained by using the hydraulic fracturing (HF) and borehole relief (BR) methods, the choice of method was based on the geological field conditions. The in-situ stress data of Huainan coalfield can not only be used to investigate local stress distribution characteristics, but also to study lithospheric stress distribution and its changing trend around the world. The World Stress Map (WSM) project is a research project that commenced in 1986 with the aim of establishing an open-access database of the present-day stress fields of the global crust (Kang et al., 2010).

In recent years, Huainan coalfield which is a major coal production area in China, has faced many problems induced by high in-situ stress, including deformation and failure of roadways and drainage boreholes (the total new length of which can be up to 7,000,000 m annually), rock bursts and coal and gas outburst. These instabilities of the underground openings induce quite low CMM capture efficiencies and have affected the mining safety. Thus it is very important to study the characteristics of the in-situ stress distribution in Huainan coalfield. In this study, first the challenges of CMM capture engineering are illustrated and then the in-situ stress measurement results of 74 test sites in 13 coal mines in Huainan coalfield are presented and discussed.

2. Background of the study area

The Huainan coalfield is located in northern Anhui Province in China. It covers 1571 km^2 and is 70 km long in the East–West direction, and 25 km long in the South–North direction (Fig. 1). The proven reserves of coal and CBM (coalbed methane) are approximately 500 $\times$ 10^8 t and 5.928 billion m^3, respectively, in Huainan coalfield above a depth of 2000 m. Huainan coalfield is a major coal production area in China, where the annual production capacity is up to 3 $\times$ 10^7 t, and the coal grade is very fine. There are between 9 and 18 mineable coal seams in Huainan coalfield, with a total thickness between 22 and 34 m. The Platts hardness coefficient and permeability of the coal seams are in the range of 0.2–0.8 and 4 $\times$ 10^{-4}–1 $\times$ 10^{-3} mD, respectively. The gas content is between 10 and 22 m^3/t, and the gas pressure can reach 6.0 MPa. The Huainan coalfield is also characterized by a complex geological structure; there are approximately 2970 faults with a throw greater than 3 m. In recent years, coal mines in Huainan coalfield have gradually entered deep mining levels as the coal source in the shallow mining levels has been exhausted. According to an incomplete statistical record (Liu and Liu, 2012; Zhang et al., 2009), the mining depth of the Xieqiao coal mine has reached 720 m, the Guqiao coal mine has reached 780 m, the Pansan coal mine and the Xinzhuangzi coal mine have reached 812 m, the Dingji coal mine has reached 860 m, and the Wangfenggan coal mine has reached 960 m.

3. CMM capture engineering challenges

Due to the high in-situ stress and the low strength of surrounding rock, roadways in the deep levels are characterized by weak stability (Fig. 2a and b). A wide zone of rock surrounding the roadway becomes broken after excavation, causing great difficulties in roadway stability control and support (He et al., 2005). The instability of the roadway and extensive development of fractures in the surrounding rock not only 1) give rise to a bad drainage borehole construction environment and a low borehole development rate, as Yao et al. (2010) showed, the success rates of boreholes drilled for gas drainage are only 90% in rock and 75% in coal seams, which also decreases gradually as the mining depths increase; but 2) also cause great difficulty in sealing drainage boreholes as cement mortar can easily flow from the fractures.

The excavation of a roadway has a significant effect on the in-situ stress distribution of the surrounding rock. At the same time, creating a drainage borehole, which is another type of underground opening, also affects the in-situ stress distribution of the surrounding rock. Thus a large number of fractures will appear around the borehole due to the disturbance superposition of multiple excavations. These fractures expand and connect over time. The distribution and development of these fractures also affects borehole sealing quality; thus, a large amount of air can flow into the borehole, leaving a very low CMM capture efficiency. In addition, the sustained development of fractures induces many stability problems of the boreholes which are usually without any support in theses coal mines. As shown in Fig. 2c–e), a partial or entire

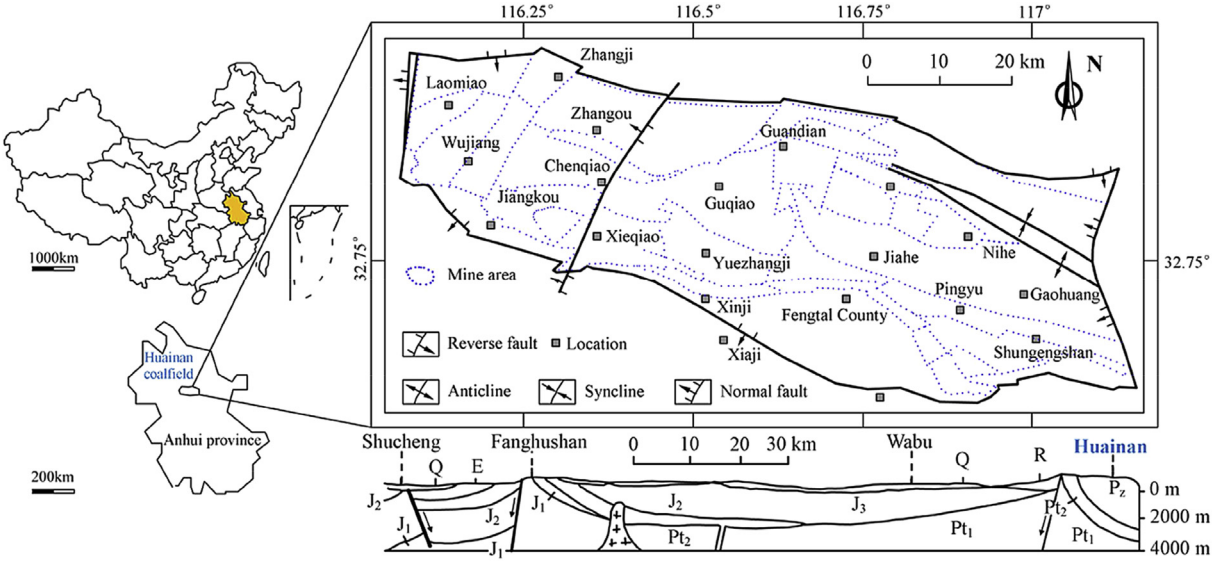

Fig. 1. Map showing the Huainan coalfield in north China.

Fig. 2. Deformation–failure of roadway and horizontal borehole in underground coal mine (Luo et al., 2010; Zhang et al., 2009).

borehole will not be able to capture CMM continually due to the deformation and failure of the surrounding rock.

In the following section, comparisons of production between two groups of drainage boreholes at the No.1331 working face (Dingji coal mine) have been made. The depth of the No.1331 working face is between 780 and 870 m. The coal seam of the No.1331 working face is characterized by very low strength; its Platts hardness coefficient is only 0.6. The average thickness and inclination angle of the coal seam is approximately 1.8 m and 3°, respectively. The gas content and gas pressure are 5.6 m^3/t and 1.2 MPa, respectively. For the sake of convenient contrast, 60 drainage boreholes with lengths of approximately 110 m have been chosen and divided into two groups. Screen pipes have been installed in these boreholes with two different methods, as these boreholes have quite low stability. The screen pipes will act as methane flow channels when failure of the borehole occurs. The traditional method was used to install screen pipes in the boreholes of the group 1, with only 60% percent of the length of these boreholes being supported by screen pipes, while nearly 100% percent the length of the boreholes of group 2 was supported by screen pipes with the new efficiency method. As shown in Fig. 3, both the concentration and flux of group 2 are larger than that of group 1. It can be concluded that borehole instability problems mainly caused by high in-situ stress and low strength of coal have extensively affected CMM capture efficiency.

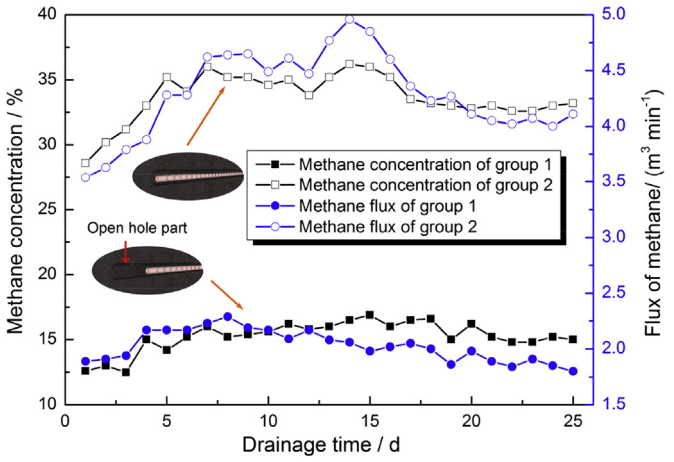

Fig. 3. Comparisons of methane concentration and flux between two groups of horizontal boreholes.

4. Results and analysis of in-situ stress

4.1. A brief review of the in-situ stress measurement methods

Methods for the determination of in-situ rock stress can be classified into two main categories, including methods that disturb the in-situ rock conditions and methods based on the observation of rock behavior without any major influence from the measuring method (Ljunggren et al., 2003). Two methods, hydraulic fracturing and borehole relief, have been widely utilized for in-situ stress measurements (Kang et al., 2010), and both belong to the first category of in-situ stress test method. The hydraulic fracturing method was first used to increase oil production, and then used by Hubbert and Willis (1957) to measure in-situ stress. Hydraulic fracturing is suitable for stress measurements in deep boreholes and can be classified into traditional hydraulic fracturing and hydraulic testing of pre-existing fractures (Haimson and Cornet, 2003). Fig. 4 illustrates the hydraulic fracturing stress test in an

underground roadway. Borehole relief is a mature and accurate method for in-situ stress measurement; however it requires better geological conditions than hydraulic fracturing (Zang et al., 2010).

4.2. In-situ stress measurement results

Huainan Mining Group Co., Ltd led the in-situ stress measurements in 11 coal mines and obtained valid results from 44 test sites. The other 30 in-situ stress measurement results from Xinjiyi coal mine and Liuzhuang coal mine were obtained from recent published studies describing a comprehensive analysis of the Huainan coalfield (Luo et al., 2011; Han and Zhang, 2009). All of the test sites were located in underground roadway. To eliminate the influence of the secondary stress distribution of the roadway on in-situ stress measurement, the lengths of the test boreholes were between 25 and 30 m. In engineering practice, the choice of the two methods was based on the geological conditions, including the integrity and inelasticity of the surrounding rock and the level of fracture development. When using the hydraulic fracturing method, a horizontal borehole was drilled in the roadway walls and vertical borehole was drilled in the roadway floor. When using the borehole relief method, horizontal borehole was drilled with a small upward angle for the sake of cleaning the test borehole. Of the 74 valid in-situ stress measurement results of Huainan coalfield that have been listed in Table 1, 60 were obtained by the hydraulic fracturing method and the others were obtained by the borehole relief method. All of the test sites were in the 350–1100 m depth range. In Table 1, σ_v is the vertical stress, MPa. σ_H is the maximum horizontal stress, MPa. σ_h is the minimum horizontal stress, MPa. λ is the coefficient of lateral stress, 1. κ is the coefficient of average lateral stress, 1. The maximum vertical stress, maximum horizontal stress and minimum horizontal stress are all obtained in Dingji coal mine at a depth of 826 m, where the three principal stresses are 36.1, 44.0 and 36.4 MPa, respectively.

Fig. 4. Photograph of hydraulic fracturing stress test in an underground roadway (Kang et al., 2010).

Among the test sites, there are 50 sites at which $\sigma_H > \sigma_v > \sigma_h$, nine sites at which $\sigma_H > \sigma_h > \sigma_v$ and 15 sites at which $\sigma_v > \sigma_H > \sigma_h$, accounting for 67.5%, 12.2% and 20.3% of the total sites, respectively. In summary, there are 59 sites at which σ_H is higher than σ_v, accounting for 79.7% of the total sites. The in-situ stress field of Huainan coalfield was formed by tectonic stress and gravity stress, with the former stress contributing a larger proportion than that of the latter. Based on the relationships of the three principal stresses, the in-situ stress field can be divided into three types (Xiang-feng and Shuang-zhong, 1998), a gravity stress field, a tectonic stress field and a latent hydrostatic stress field. In the gravity stress field, the in-situ stress is mainly formed by the mass of the overlying rock. The maximum principal stress is mainly vertical stress that is approximately equal to γH, where γ is the average specific weight of the overlying rock, kN/m^3, and H is the thickness of the overlying rock, m. The intermediate and minimum principal stresses are mainly horizontal stress. In the tectonic stress field, the in-situ stress is formed by tectonic stress and gravity stress, and the maximum principal stress is mainly horizontal stress. The latent hydrostatic stress field is characterized by the hydrostatic pressure, i.e., the three principal stresses are approximately equal to each other due to the characteristics of rock and increasing depth of burial. According to the classifications, the stress field of Huainan coalfield in the 350–1100 m depth range belongs to the tectonic stress field.

Among the 74 measurement results, 55 have records of the orientation of the maximum horizontal principal stress, while the measurement results of the Xinji coal mine have incomplete records of the orientation of the maximum horizontal principal stress. The explanation of the orientation of the maximum horizontal principal stress in Huainan coalfield was based on the 55 measurement results for a compromise approach. The orientation of the maximum horizontal principal stress of 47 of the measurements is in the range of N0.0°E to N90.0°E, and 25 measurements were in the range of N80.0°E to N90.0°E, accounting for 84.45% and 45.45% respectively. The orientation of the horizontal principal stress of Huainan coalfield is mainly along the NEE–EW direction.

It is clear that the orientation and magnitude of the maximum horizontal principal stress varies with the time and space (Shengrui, 2001). A brief analysis of the maximum horizontal principal stress with respect to the burial history and geological structure of Huainan coalfield is needed. Huainan coalfield mainly experienced Indosinian movement, Yanshan movement and Himalayan movement (Jiang et al., 1992; Liu and Lu, 2010). The maximum horizontal principal stress was influenced by the superimposition effect of the three geological conformation movements, and the strongest influence was generated by the Himalayan movement. The Panji anticline at 17 km long and 1.6 km wide is the main geological structure of Huainan coalfield, the axial orientation of which is along the N70.0°W direction (Ye et al., 2011; Le et al., 2011) Moreover, the faults widely distributed in Huainan coalfield are along the NE and NNE direction (Han and Zhang, 2009; Song et al., 2005). The results of Hudson and Cooling (1988) show that the orientation of the maximum horizontal principal stress will be parallel to the structural plane of the geological structure when the structural plane is open, and will be perpendicular to the structural plane of the geological structure when the structural plane is closed. It can be concluded that the orientation of the maximum horizontal principal stress is mainly perpendicular to the Panji

Table 1
Results of in-situ stress in Huainan coalfield.

No.	Coal mine name	Depth (m)	σ_v (MPa)	σ_H (MPa)	σ_h (MPa)	Orientation of σ_H	λ	κ	Method
1	Dingji	826.00	36.10	44.00	36.40	N52.0°E	1.22	1.11	HF
2	Gubei	648.00	17.80	19.07	17.03	N32.0°E	1.07	1.01	BR
3	Guqiao	780.00	17.57	19.76	16.12	N60.2°W	1.12	1.02	BR
4	Guqiao	827.00	18.04	29.50	17.12	N83.0°E	1.64	1.29	HF
5	Guqiao	829.00	18.08	30.71	17.75	N83.0°E	1.70	1.34	HF
6	Liuzhuang	768.00	19.25	23.65	12.32	N90.0°E	1.23	0.93	HF
7	Panbei	490.00	12.90	20.30	11.80	N59.1°W	1.57	1.24	BR
8	Paner	502.00	11.44	20.85	11.62	N84.0°E	1.82	1.42	HF
9	Paner	535.80	12.14	20.64	10.84	N83.0°E	1.70	1.30	HF
10	Paner	537.80	12.36	20.20	10.99	N84.0°E	1.63	1.26	HF
11	Paner	550.00	16.47	13.43	7.22	N78.9°E	0.82	0.63	BR
12	Pansan	735.00	18.38	16.24	8.52	N84.7°E	0.88	0.67	HF
13	Pansan	750.00	20.10	23.62	11.67	N87.6°W	1.18	0.88	BR
14	Pansan	770.00	20.10	23.62	11.67	N87.6°E	1.18	0.88	HF
15	Panyi	740.00	18.50	19.85	10.38	N33.3°E	1.07	0.82	HF
16	Panyi	750.00	19.65	21.60	17.02	N79.2°W	1.10	0.98	BR
17	Panyi	785.00	17.31	28.33	16.33	N83.0°E	1.64	1.29	HF
18	Panyi	549.00	13.21	23.06	12.18	N22.8°W	1.75	1.33	BR
19	Panyi	543.00	15.15	17.14	10.98	N55.4°E	1.13	0.93	BR
20	Panyi	793.00	17.31	28.33	16.33	N83.0°E	1.64	1.29	HF
21	Wangfenggang	842.00	18.46	20.22	11.78	N80.0°E	1.10	0.87	HF
22	Wangfenggang	843.30	18.52	20.11	11.78	N79.0°E	1.09	0.86	HF
23	Wangfenggang	844.20	18.58	18.67	11.20	N81.0°E	1.00	0.80	HF
24	Wangfenggang	981.00	21.48	24.07	12.38	N82.0°E	1.12	0.85	HF
25	Wangfenggang	983.20	21.63	23.39	12.07	N83.0°E	1.08	0.82	HF
26	Wangfenggang	984.70	21.71	22.68	11.93	N83.0°E	1.04	0.80	HF
27	Wangfenggang	817.00	23.96	20.33	17.13	N8.4°E	0.85	0.78	BR
28	Wangfenggang	820.00	19.90	22.88	20.42	N31.7°E	1.15	1.09	BR
29	Xieyi	803.00	20.08	16.90	8.93	N46.2°W	0.84	0.64	HF
30	Xieyi	780.00	14.50	20.54	13.76	N26.4°E	1.42	1.18	BR
31	Xieyi	837.00	18.46	20.22	11.78	N80.0°E	1.10	0.87	HF
32	Xieyi	981.00	21.48	24.07	12.38	N82.0°E	1.12	0.85	HF
33	Xieyi	983.20	21.63	23.39	12.07	N82.0°E	1.08	0.82	HF
34	Xieyi	673.00	17.78	25.20	12.89	N64.0°E	1.42	1.07	BR
35	Xieyi	793.00	21.37	31.20	17.89	N67.8°E	1.46	1.15	BR
36	Xinjiyi	757.60	20.64	19.37	14.84	N55.0°E	0.94	0.83	HF
37	Xinjiyi	350.70	9.47	14.20	9.50	N53.0°E	1.50	1.25	HF
38	Xinjiyi	373.60	10.09	10.10	7.72	N49.0°E	1.00	0.88	HF
39	Xinjiyi	666.60	18.00	10.36	9.86	N52.0°E	0.58	0.56	HF
40	Xinjiyi	555.18	14.99	18.78	13.52	–	1.25	1.08	HF
41	Xinjiyi	589.74	15.92	16.74	12.84	–	1.05	0.93	HF
42	Xinjiyi	652.72	17.62	23.52	16.52	–	1.33	1.14	HF
43	Xinjiyi	718.64	19.40	20.78	15.28	–	1.07	0.93	HF
44	Xinjiyi	845.10	22.82	25.97	18.84	–	1.14	0.98	HF
45	Xinjiyi	460.10	12.42	14.90	10.20	–	1.20	1.01	HF
46	Xinjiyi	553.46	14.94	26.63	16.53	–	1.78	1.44	HF
47	Xinjiyi	632.63	17.08	8.63	7.93	–	0.51	0.48	HF
48	Xinjiyi	440.00	13.20	13.10	12.16	–	0.99	0.96	HF
49	Xinjiyi	470.00	14.10	14.01	13.52	N86.1°E	0.99	0.98	HF
50	Xinjiyi	485.00	14.55	14.28	13.57	–	0.98	0.96	HF
51	Xinjiyi	512.00	15.36	15.00	14.82	–	0.98	0.97	HF
52	Xinjiyi	540.00	16.20	16.12	15.61	N67.2°E	1.00	0.98	HF
53	Xinjiyi	560.00	16.80	16.50	15.06	–	0.98	0.94	HF
54	Xinjiyi	580.00	17.40	20.22	17.55	–	1.16	1.09	HF
55	Xinjiyi	600.00	18.00	21.82	18.01	N87.7°W	1.21	1.11	HF
56	Xinjiyi	620.00	18.60	24.15	19.91	–	1.30	1.18	HF
57	Xinjiyi	640.00	19.20	24.83	19.24	N79.8°E	1.29	1.15	HF
58	Xinjiyi	500.00	15.00	14.80	12.16	–	0.99	0.90	HF
59	Xinjiyi	535.00	16.05	18.72	15.52	N66.1°E	1.17	1.07	HF
60	Xinjiyi	580.00	17.40	17.73	15.57	–	1.02	0.96	HF
61	Xinjiyi	665.00	19.95	21.47	17.82	–	1.08	0.98	HF
62	Xinjiyi	715.00	21.45	22.67	20.64	N89.2°E	1.06	1.01	HF
63	Xinjiyi	790.00	23.70	24.50	21.16	–	1.03	0.96	HF
64	Xinjiyi	820.00	24.60	24.67	22.30	–	1.00	0.95	HF
65	Xinjiyi	745.00	25.35	25.64	23.10	N77.7°W	1.01	0.96	HF
66	Xinzhuangzi	623.00	14.33	15.74	8.19	N66.0°E	1.10	0.83	HF
67	Xinzhuangzi	627.00	14.42	15.92	8.61	N64.0°E	1.10	0.85	HF
68	Xinzhuangzi	629.00	14.47	17.00	9.46	N65.0°E	1.17	0.91	HF
69	Xinzhuangzi	623.00	14.33	15.74	8.19	N85.0°E	1.10	0.83	HF
70	Xinzhuangzi	627.00	14.42	15.92	8.61	N85.0°E	1.10	0.85	HF
71	Xinzhuangzi	629.00	14.47	17.00	9.46	N85.0°E	1.17	0.91	HF
72	Xinzhuangzi	650.00	19.50	15.70	12.80	N 0.0°E	0.81	0.73	BR
73	Zhangji	1076.00	26.89	27.73	19.84	N67.0°E	1.03	0.88	HF
74	Zhangji	1041.00	26.01	28.57	13.49	N64.2°E	1.10	0.81	HF

anticline and the major faults. The orientation of the maximum horizontal principal stress is closely related to the major geological structure in Huainan coalfield, further validating that the stress field of Huainan coalfield in the 350–1100 m depth range belongs to the tectonic stress field.

5. Relationships of in-situ stress variation with depth

5.1. Principal stress magnitude variation with depth

The relationships of the change in the three principal stresses to variation in the depth of Huainan coalfield in the 350–1100 m depth range are shown in Fig. 5. The scatter plot of the three principal stresses has certain regularity, i.e., the vertical stress results are distributed between the maximum and minimum horizontal stress results. The blue straight line represents a linear regression analysis of the stress measurement results of vertical stress. The gray straight line is the relationship of vertical stress variation with depth, and is the result of 116 in-situ measurement results from around the world obtained and summarized by Brown and Hoek (1978), i.e., $\sigma_v = 0.027H$. It is not considered suitable to establish linear relationships between the two horizontal principal stresses and depth as the stress field of Huainan coalfield in the 350–1100 m depth range belongs to the tectonic stress field. As shown in Fig. 5, the upper limit and lower limit of the two horizontal principal stresses were introduced to give a further explanation of the relationship between the variation of the two horizontal stresses and depth. The upper limit and lower limit were derived to cover most of the horizontal stress results (Zang et al., 2010; Wilson, 1983).

The depth range was divided into four groups for a clearer analysis of the variation of the three principal stresses with depth.

[1] There are 23 test sites in the 350–600 m depth range; at 15 sites, σ_H is larger than σ_v, and at 19 sites, σ_v is larger than σ_h, accounting for 65.2% and 82.6% of the total sites, respectively.
[2] There are 32 sites in the 600–800 m at 27 sites, σ_H is larger than σ_v, and at 29 sites, σ_v is larger than σ_h, accounting for 84.4% and 90.6% of the total sites, respectively.
[3] There are 17 sites in the 600–800 m depth range; at 15 sites, σ_H is larger than σ_v, and at 15 sites, σ_v is larger than σ_h, accounting for 88.2% and 88.2% of the total sites, respectively.
[4] There are 2 sites below a depth of 1000 m; at all sites, σ_H is larger than σ_v, and σ_v is larger than σ_h.

Table 2
Distribution of in-situ stress in Huainan coalfield.

Depth/m	$\sigma_H > \sigma_v > \sigma_h$	$\sigma_H > \sigma_h > \sigma_v$	$\sigma_v > \sigma_H > \sigma_h$	Total
350–600	11 (47.8%)	4 (17.4%)	8 (34.8%)	23
600–800	24 (75%)	3 (9.4%)	5 (15.6%)	32
800–1000	13 (76.4%)	2 (11.8%)	2 (11.8%)	17
>1000	2 (100%)	0 (0)	0 (0)	2
Total	50 (67.6%)	9 (12.2%)	15 (20.2%)	74

Note: Values within parentheses indicate the percentage of the magnitude of the three principal stresses for each depth range.

In-situ stress results of the above mentioned four depth ranges are listed in Table 2.

It can be concluded that:

[1] The percentage of the sites at which σ_H is greater than σ_v increase from 65.2% to 100% as the depth increases. However, the percentage of the sites at which σ_v is greater than σ_h has no obvious relationship to depth.
[2] It is clear that all three principal stresses increasing with depth. The rate of σ_v increasing with depth in Huainan coalfield is lower than that obtained by Brown and Hoek in their global analysis.
[3] The maximum and minimum principal stresses are mainly horizontal stress, and the intermediate principal stress is mainly vertical stress.
[4] The upper and lower limits for the maximum horizontal stress are $\sigma_H = 0.0335H + 4.621$ and $\sigma_H = 0.0101H + 8.721$ respectively; for the minimum horizontal stress these limits are $\sigma_h = 0.0201H + 4.116$ and $\sigma_h = 0.0064H + 3.728$ respectively. Most scatter data of maximum and minimum horizontal stresses occurs within the range defined by their upper and lower limits, respectively. Most scatter data of maximum horizontal stress is located upon the regression line of vertical stress, which is consistent with indicating a characteristic of the tectonic stress field.

5.2. Coefficient of lateral stress variation with depth

The coefficient of lateral stress, λ, is of great significance representing a key characteristic of in-situ stress distribution. It is defined as the ratio of the maximum horizontal principal stress to

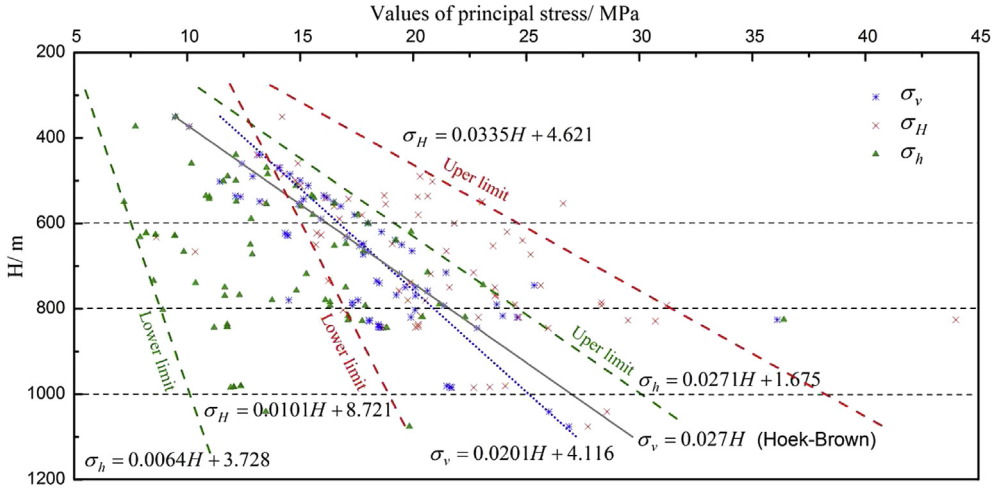

Fig. 5. Values of in-situ principal stresses vs. depth in Huainan coalfield.

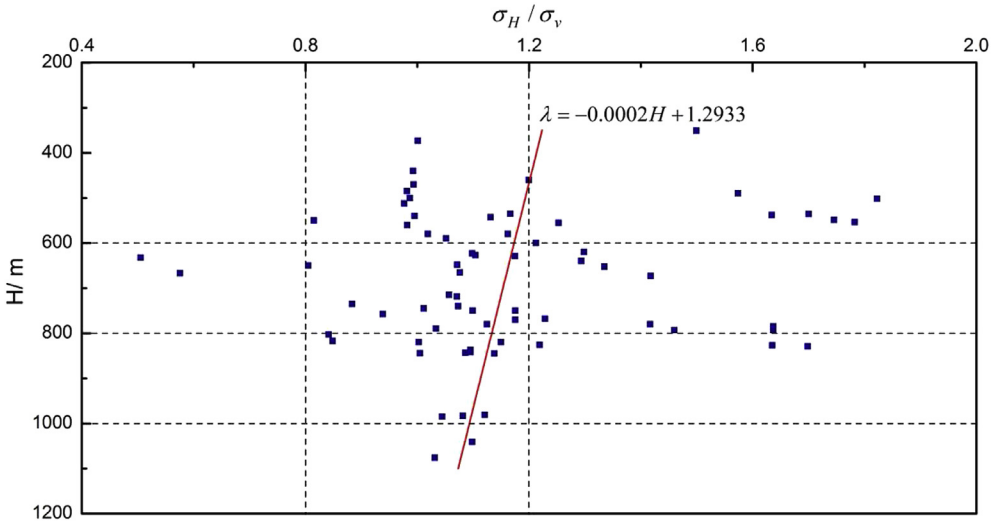

Fig. 6. Variation of the coefficient of lateral stress with depth.

vertical stress. The relationship between the coefficient of lateral stress and depth of Huainan coalfield in the 350–1100 m depth range are shown in Fig. 6. λ falls in the range of 0.51–1.82 and decreases gradually as depth increases.

λ was divided into three groups, as listed in Table 3. There are only two sites at which λ is smaller than 0.8, 21 sites at which λ is larger than 1.2 and 51 sites at which λ is in the range of 0.8–1.2, accounting for 2.7%, 28.4% and 68.9% of the total sites, respectively. The percentage of the sites at which λ is in the range of 0.8–1.2 increases gradually with depth. It can then be surmised that λ gradually approaches 1.0, implying that hydrostatic pressure may occur in deep levels of Huainan coalfield.

5.3. Coefficient of average lateral stress variation with depth

The relationship between the variation of the coefficient of average lateral stress and depth in the Huainan coalfield in the 350–1100 m depth range is shown in Fig. 7. The coefficient of average lateral stress, κ, is the ratio of the average horizontal principal stress to vertical stress, which is in the range of 0.48–1.44. The average horizontal principal stress can be estimated from the maximum and minimum horizontal principal stresses.

$$\kappa = \frac{\sigma_H + \sigma_h}{2\sigma_v} \tag{1}$$

Hoed and Brown (Brown and Hoek, 1978) summarize in-situ stress measurement results from around the world and found that the coefficient of average lateral stress, κ, generally lies within limits defined by

$$\frac{100}{H} + 0.3 \le \kappa \le \frac{1500}{H} + 0.5 \tag{2}$$

The average value of κ can be deduced as follows:

$$\kappa = \frac{800}{H} + 0.4 \tag{3}$$

It can be found that κ has a linear relation with the reciprocal of the depth, i.e. when $x = 1/H$, we have

$$\kappa = ax + b \tag{4}$$

where a and b are fitting coefficients and can be obtained from the linear regression analysis of the stress measurement results. After calculation, Eq. (4) can be written as:

$$\kappa = \frac{129.4}{H} + 0.7793 \tag{5}$$

As shown in Fig. 7, κ decreases gradually with the increasing depth, and rate of the decrease reduces simultaneously. The green curve is the characteristic curve of the left part of Eq. (2) and is called the Hoek–Brown outer envelope; the red curve is the characteristic curve of Eq. (3) and is called the Hoek–Brown median envelope; and the blue curve is the characteristic curve of Eq. (5). It is clear that the blue curve is located between the other two characteristic curves, and its variation trend is similar to that of the green curve. The coefficient of average lateral stress of Huainan coalfield in the 350–1100 m depth range is within the range defined by the Hoek–Brown outer envelope and the Hoek–Brown median envelope.

Table 3
Distribution of the coefficient of lateral stress in Huainan coalfield.

Depth/m	<0.8		0.8–1.2		>1.2		Total
	Numbers	Percent/%	Numbers	Percent/%	Numbers	Percent/%	
350–600	0	0	15	65.2	8	34.8	23
600–800	2	6.2	20	62.5	10	31.3	32
800–1000	0	0	14	82.4	3	17.6	17
>1000	0	0	2	100	0	0	2
Total	2	2.7	51	68.9	21	28.4	74

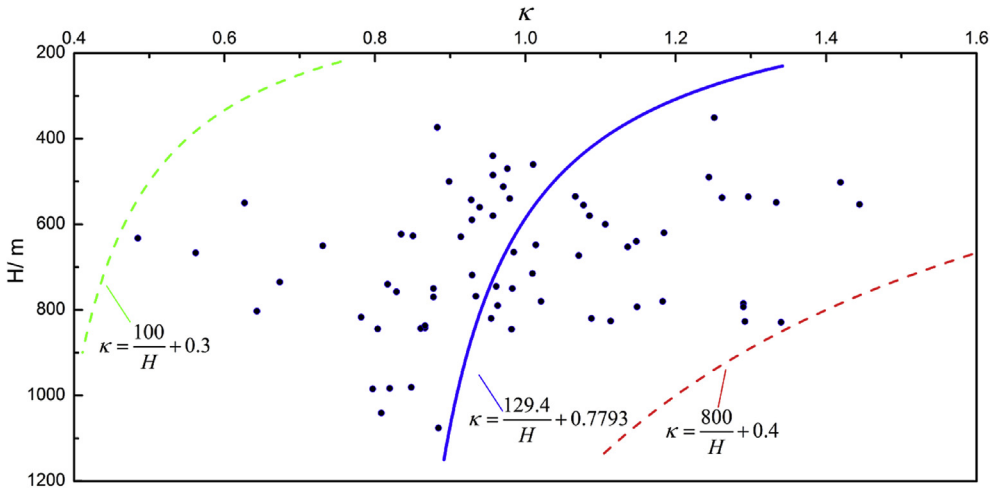

Fig. 7. Coefficient of the average lateral stress variation with depth.

6. Discussion of the stability of underground openings

In the deep mining levels, the rock is in a complex geological environment that is characterized by high in-situ stress, high temperature and high osmotic pressure, making it quite different from that found in the shallow levels in both organizational structure and basic mechanical behavior (Liu and Lu, 2010). In particular, the rock in the shallow levels is mostly in the elastic state and is characterized by stiffness and stability, while in the deep levels it is mostly in latent plastic or plastic state and is characterized by softness and stretchability (Quansheng et al., 2004).

Underground openings may fail when the surrounding stress exceeds the tensile, compressive, or shear strengths of the rock formation, whichever is reached first (Zhang et al., 2003). Among the various available failure criteria, the Mohr–Coulomb criterion is the most commonly used failure criterion to estimate borehole wall stability. Based on the Mohr–Coulomb criterion, the following expressions of tangential stress σ_r^{p} and radial stress $\sigma_\theta^{\mathrm{p}}$ can be obtained for the stresses that exceed the yield strength (i.e., plastic status) around the underground opening (Wang et al., 2012b):

$$\begin{cases} \sigma_r^{\mathrm{p}} = \dfrac{q}{\varepsilon-1}\left[\left(\dfrac{r}{r_{\mathrm{a}}}\right)^{\varepsilon-1}-1\right]+P_i\left(\dfrac{r}{r_{\mathrm{a}}}\right)^{\varepsilon-1} \\ \sigma_\theta^{\mathrm{p}} = \dfrac{q}{\varepsilon-1}\left[\varepsilon\left(\dfrac{r}{r_{\mathrm{a}}}\right)^{\varepsilon-1}-1\right]+\varepsilon P_i\left(\dfrac{r}{r_{\mathrm{a}}}\right)^{\varepsilon-1} \\ q = 2c\sqrt{\varepsilon} \\ \varepsilon = \dfrac{1+\sin\varphi}{1-\sin\varphi} \end{cases} \tag{6}$$

where q and ε are intermediate variables. c is the cohesion of coal, MPa. φ is the internal frictional angle, rad. P_i is the borehole pressure, MPa. r_{a} is the radius of the borehole, m. r is the distance from the center of the underground opening, m. As shown in Fig. 8, both the tangential stress and the radial stress change with the distance from the center of the underground opening. Rock surrounding the underground opening is characterized by elastic–plastic secondary stress distribution. The tangential stress increases with increasing r, and the radial stress first increases then decreases with increasing r. Therefore according to the Mohr–Coulomb criterion, there must be a distance R_{p} at which we have

$$\sigma_\theta^{\mathrm{p}} = \sigma_\theta^{\mathrm{e}} \tag{7}$$

where $\sigma_\theta^{\mathrm{e}}$ is the radial stress of the coal which is in an elastic state, MPa. The point at a distance from the center of the borehole R_{p} is generally considered as the plastic zone radius, and it can be deduced as:

$$R_{\mathrm{p}} = r_{\mathrm{a}}\left[\frac{2}{\varepsilon+1}\,\frac{P_0(\varepsilon-1)+q}{P_i(\varepsilon-1)+q}\right]^{1/(\varepsilon-1)} \tag{8}$$

where P_0 is the initial in-situ stress, MPa.

According to theoretical analysis, many factors influence the stability of underground openings, including the initial in-situ stress status (which includes the values of the three principal stresses, coefficients of average lateral stress and average lateral stress), coal or rock strength, gas pressure, support pattern and strength. The in-situ stress distribution is one of the most important fundamental factors affecting the stability of underground openings (Zang et al., 2010).

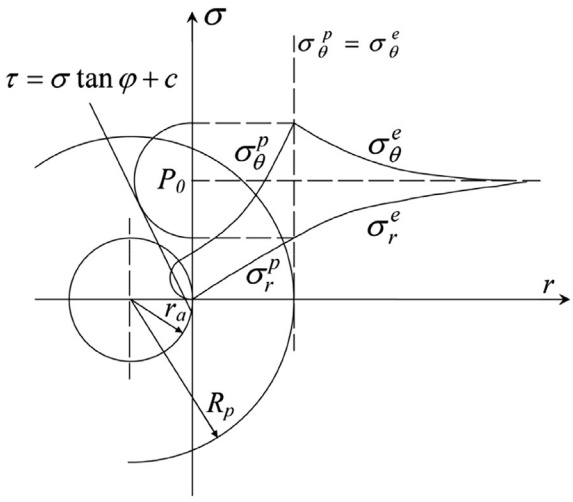

Fig. 8. Illustration of elastic–plastic secondary stress distribution around an underground opening.

7. Conclusions

In this study, the challenges for CMM capture Engineering caused by the instability of underground openings in deep mining levels of Huainan coalfield have been discussed. In-situ stress distribution is one of the most important and fundamental factors affecting the stability of underground openings. Additionally, the in-situ stress measurement results of 74 test sites in 13 coal mines have been analyzed to enhance our understanding of the characteristics of in-situ stress distribution in deep mining levels of Huainan coalfield. Based on the work completed, the following conclusions are made:

[1] Among 74 test sites, there are 59 sites, at which σ_H is larger than σ_v, accounting for 79.7% of the total sites. The orientation of the maximum horizontal principal stress of 47 measurements is in the range of N0.0°E to N90.0°E, and for 25 measurements is in the range of N80.0°E to N90.0°E, accounting for 84.45% and 45.45%, respectively. The orientation of the horizontal principal stress of Huainan coalfield is mainly along the NEE–EW direction. The in-situ stress field of Huainan coalfield in the range of 350–1100 m belongs to the tectonic stress field which is formed by tectonic stress and gravity stress, with the former stress contributing a larger proportion than that of the latter. The orientation of the maximum horizontal principal stress is closely related to the major geological structure in Huainan coalfield, further validating that the stress field of Huainan coalfield in the 350–1100 m depth range belongs to the tectonic stress field.

[2] The three principal stresses all increase with depth. The increase rate of σ_v with depth in Huainan coalfield is smaller than that outlined in a global study. The maximum and minimum principal stresses are mainly horizontal stress, and the intermediate principal stress is mainly vertical stress.

[3] The coefficients of the lateral stress of Huainan coalfield range from 0.51 to 1.82 and decrease gradually with depth, having a trend approaching 1.0, implying that hydrostatic pressure may occur in deep levels of Huainan coalfield.

[4] The coefficients of average lateral stress of Huainan coalfield range from 0.48 to 1.44 and decrease gradually with depth. The relationship between depth and κ can be expressed as $\kappa = 129.4/H + 0.7793$, the characteristic curve of which is located between the Hoek–Brown outer envelope and the Hoek–Brown median envelope. The variation trend of the characteristic curve is similar to that of Hoek–Brown outer envelope.

Acknowledgments

This work was supported by the Natural Science Foundation for the Youth of China (No.51304204, No.51204173), Natural Science Foundation of China (No.51374204), and the Basic Research Program of Huainan Mining Group Co., Ltd (HNKY- KT- (2013)- 003).

References

Bell, J., 2003. Practical methods for estimating in situ stresses for borehole stability applications in sedimentary basins. J. Petrol. Sci. Eng. 38, 111–119.
Bibler, C.J., Marshall, J.S., Pilcher, R.C., 1998. Status of worldwide coal mine methane emissions and use. Int. J. Coal Geol. 35, 283–310.
Brown, E., Hoek, E., 1978. Trends in relationships between measured in-situ stresses and depth. In: International Journal of Rock Mechanics and Mining Sciences & Geomechanics Abstracts. Pergamon, pp. 211–215.
Haimson, B., Cornet, F., 2003. ISRM suggested methods for rock stress estimation—part 3: hydraulic fracturing (HF) and/or hydraulic testing of pre-existing fractures (HTPF). Int. J. Rock Mech. Min. Sci. 40, 1011–1020.
Han, J., Zhang, H., 2009. Characteristic of in-situ stress field in Huainan mining area. Coal Geol. Explor. 1, 004.
He, M.C., Xie, H., Peng, S., Jiang, Y., 2005. Study on rock mechanics in deep mining engineering. Chin. J. Rock Mech. Eng. 24, 2803–2813.
Hubbert, M.K., Willis, D.G., 1957. Mechanics of Hydraulic Fracturing.
Hudson, J., Cooling, C., 1988. In situ rock stresses and their measurement in the UK—Part I. The current state of knowledge. In: International Journal of Rock Mechanics and Mining Sciences & Geomechanics Abstracts. Elsevier, pp. 363–370.
Jiang, B., Wang, G., Gao, Y., 1992. Characteristics of microscopic deformation and mechanism of the Fengyang-Fengtai nappe in the Yingshan-Fengtai area, Huainan coalfield, Anhui. Region. Geol. China 1, 60–67 (in Chinese).
Kang, H.-P., Zhang, X., Si, L.-P., Wu, Y., Gao, F., 2010. In-situ stress measurements and stress distribution characteristics in underground coal mines in China. Eng. Geol. 116, 333–345.
Karacan, C.Ö., Ruiz, F.A., Cotè, M., Phipps, S., 2011. Coal mine methane: a review of capture and utilization practices with benefits to mining safety and to greenhouse gas reduction. Int. J. Coal Geol. 86, 121–156.
Le, Q., Lin, C., Miao, X., Ye, Z., 2011. The relationship between the Panji anticline and the development characteristics and distribution laws of interlayer-gliding structure in seams. In: Electrical and Control Engineering (ICECE), 2011 International Conference on, IEEE, pp. 1835–1838.
Li, H., Fu, K., 2006. Some major technical problems and countermeasures for deep mining. J. Min. Saf. Eng. 23, 468–471.
Liu, Q.-S., Lu, X.-L., 2010. Research on nonlinear large deformation and support measures for broken surrounding rocks of deep coal mine roadway. Rock Soil Mech. 10, 040.
Liu, Q.-S., Liu, K.-D., 2012. Characteristics of in-situ stress field for deep levels in Huainan coal mine. Rock Soil Mech. 7, 027.
Ljunggren, C., Chang, Y., Janson, T., Christiansson, R., 2003. An overview of rock stress measurement methods. Int. J. Rock Mech. Min. Sci. 40, 975–989.
Luo, C., . Li, H., Liu, Y., 2010. Study of distributing characteristics of stress in surrounding rock masses and in-situ stress measurement for deeply buried tunnels. Chin. J. Rock Mech. Eng. 7, 018.
Luo, C., . Li, H., Liu, Y., 2011. Characteristics of in-situ stress and variation law of plastic zone of surrounding rocks around deep tunnels in a coal mine. Chin. J. Rock Mech. Eng. 8, 014.
Martin, C., Kaiser, P., Christiansson, R., 2003. Stress, instability and design of underground excavations. Int. J. Rock Mech. Min. Sci. 40, 1027–1047.
Moos, D., Peska, P., Zoback, M., 1998. Predicting the stability of horizontal wells and multi-laterals: the role of in situ stress and rock properties. In: SPE International Conference on Horizontal Well Technology, pp. 119–130.
Peška, P., Zoback, M.D., 1995. Compressive and tensile failure of inclined well bores and determination of in situ stress and rock strength. J. Geophys. Res. Solid Earth 100, 12791–12811 (1978–2012).
Quansheng, L., Hua, Z., Tao, L., 2004. Study on stability of deep rock roadways in coal mines and their support measures. Chin. J. Rock Mech. Eng. 23, 3732–3737.
Shengrui, S., 2001. The Effect of Fractures on Rock Stresses and its Significance in Geological Engineering. Chendu University of Technology, Chengdu.
Song, C.-Z., Zhu, G., Liu, G.-S., Niu, M.-L., 2005. Identificating of structure and its dynamics control of Huainan coalfield. Coal Geol. Explor. 1, 003.
Wan, W., Raj, A., Hsu, T., Lohateeraparp, P., Harwell, J.H., Shiau, B., 2013. Designing surfactant-only formulations for a high salinity and Tight Reservoir. Int. News Fats Oils Relat. Mater. 24 (10), 622–627.
Wang, L., Cheng, Y.-P., Wang, L., Guo, P.-K., Li, W., 2012a. Safety line method for the prediction of deep coal-seam gas pressure and its application in coal mines. Saf. Sci. 50, 523–529.
Wang, F., Ren, T., Tu, S., Hungerford, F., Aziz, N., 2012b. Implementation of underground longhole directional drilling technology for greenhouse gas mitigation in Chinese coal mines. Int. J. Greenhouse Gas Control 11, 290–303.
Wilson, A.H., 1983. The stability of underground workings in the soft rocks of the coal measures. Int. J. Min. Eng. 1, 91–187.
Xiang-feng, P., Shuang-zhong, Y., 1998. General type of in-situ stress field in Huainan mine area. J. China Univ. Min. Technol. 27, 60–63.
Yao, X.-R., Cheng, Gong-lin, Shi, Bi-ming, 2010. Analysis on gas extraction drilling instability and control method of pore-forming in deep surrounding-rock with weak structure. J. China Coal Soc. 35, 2073–2081.
Yao, Y., Liu, D., Tang, D., Tang, S., Huang, W., Liu, Z., Che, Y., 2009. Fractal characterization of seepage-pores of coals from China: an investigation on permeability of coals. Comput. Geosci. 35, 1159–1166.
Yuan, L., 2008. Theory and Practice of Integrated Pillarless Coal Production and Methane Extraction in Multiseams of Low Permeability. China Coal Industry Publishing House.
Ye, Z., Le, Q.-L., Lin, C.-H., 2011. Controlling effect of Panji anticline on mine interlayer-gliding structure. Coal Technol. 9, 067.
Zang, A., Stephansson, O., Stephansson, O., 2010. Stress Field of the Earth's Crust. Springer.
Ze, Z., Sx, J., 2014. Hollow fiber membrane contactor absorption of CO2 from the flue gas: review and perspective. Glob. Nest J. 16, 355–374.
Zhang, J., Bai, M., Roegiers, J.C., 2003. Dual-porosity poroelastic analyses of wellbore stability. Int. J. Rock Mech. Min. Sci. 40, 473–483.
Zhang, B.-H., Li-jun, H., Gui-lei, H., 2008. Study of 3D in-situ stress measurement and stability of roadways in depth. Rock Soil Mech. 29, 2547–2551.
Zhang, N., Wang, C., Gao, M., Zhao, Y., 2009. Roadway support difficulty classification and controlling techniques for Huainan deep coal mining. Chin. J. Rock Mech. Eng. 12, 010.